International Journal of Research in Engineering and Science (IJRES)
ISSN (Online): 2320-9364, ISSN (Print): 2320-9356
www.ijres.org Volume 10 Issue 9 ǁ September 2022 ǁ PP. 130-144

Numerical modeling by finite elements of a cylindrical pressure vessel made of composite material

Diana Yulieth Soto Pineda, *disotop@unal.edu.co, Mechanical Engineer, Master student, National University of Colombia,*
Jairo Andrés Paredes López, *japaredesl@unal.edu.co Ph.DCivil engineering Deparment, National University of Colombia*

ABSTRACT: *Pressure vessels are used to perform various services, from storing gases at high pressures, transporting liquids, heat exchangers, pipes, fuel tanks, fuselages, boilers, among others, steel is commonly the material used for its fabrication. At present, composite materials are being studied, which present high resistance, without corrosion problems and low weight. In a composite material, there is a simple material that is lighter and more resistant than acts as a matrix, and joins with fiber material of greater resistance, their combination gives rise to the composite. This research thesis studies the stresses experienced by a vertical cylindrical pressure vessel, made of a composite material of aluminum metal matrix and boron fibers, and compares it with a steel vessel. Two models were created for parameter calibration, with the theory of series/parallel mixtures (SP), the composite material was designed and the efforts were estimated theoretically, which were later compared with the results obtained in the finite element analysis tools in APDL. From the results, a better performance of the pressure vessel in composite material was identified compared to the steel pressure vessel, a reduction in total weight was estimated in the model in composite material compared to the model in steel and additionally the vulnerability to corrosion was eliminated. Finally, it is concluded that the objectives proposed at the beginning of the investigation were met, providing an analysis methodology that applies theory with numerical modeling together for the analysis and can be easily replicated by other studies.*
KEYWORDS: *pressure vessel, composite materials, membrane theory of shells, theory of series/parallel mixtures*

Date of Submission: 25-08-2022 Date of acceptance: 09-09-2022

I. INTRODUCTION

Cylindrical pressure vessels are widely used in the fluid transportation industry, fuel storage tanks, aircraft fuselages, heat exchangers, among others. The pressure vessel must, therefore, have high mechanical resistance and, depending on the environmental conditions of exposure, also high resistance to corrosion. Usually made of alloy steel, this homogeneous material is resistant to pressure loading, however, it adds a great deal of weight and is vulnerable to corrosion. An alloy steel container translates into greater handling difficulty, higher energy consumption and mechanical failures due to corrosion. To respond to the specific operating needs of this type of structure and to solve the problems that arise when using the conventionally used simple material, the design of light and resistant materials is necessary, it is there where composite materials become a viable answer [1]. Composite materials are designed under the requirements of the project where they will be used, unlike conventional homogeneous simple materials, these allow controlling factors such as mechanical behavior and the final weight that they will contribute to the project.

This research thesis is an academic exercise developed in order to provide the stress analysis in the cylindrical zone of a pressure vessel made of steel and a pressure vessel made of composite material, in order to compare the performance of both [2]. Initially, two parameter calibrations were performed using simple numerical models. The first calibration was carried out to design the composite material. Using the series/parallel (SP) mixing theory, the constitutive matrix of the three-layer anisotropic composite material of fiber orientation at +37°, -37°, +18° was theoretically obtained [3]. This material was assigned to a simple numerical model of a beam created in APDL (ANSYS Parametric Design Language).

The second calibration was performed to verify the assignment of the cylindrical coordinate system to the finite elements and the coherence of the stress results [4]. A simple numerical model of a cylindrical section in APDL was created following a typical finite element modeling process (figure 1), it was assigned the theoretically designed composite material in the first calibration and the shell membrane theory was used to obtain the theoretical stresses to compare them with those obtained in the numerical modeling [5].Due to the

reliability achieved in the calibrations, it was decided to proceed with the design of the cylindrical pressure vessel.

A commercial geometry of a Y-oriented vertical cylindrical pressure vessel was selected [6]. The selected geometry is of a thin-walled cylindrical pressure vessel that stores hydrogen, a gas that is widely used industrially. Hydrogen is essential in the aerospace industry as fuel for rocket engines, in the supply of energy to equipment and life support systems, it can be stored as a liquid, gas or chemical compound, it is converted into energy through traditional combustion methods (in engines, furnaces or gas turbines), through electrochemical processes (in fuel cells) and through hybrid approaches such as integrated, it is used as a raw material or fuel in oil refining, ammonia production, among others [7].

Thus, a widely used and commercially valid geometry was chosen. In APDL, the numerical model of the pressure vessel was created according to the selected geometry, a pressure of 15 MPa was assigned to it, which is the working pressure of the commercial vessel that stores hydrogen, and the movement in Y at the base of the vessel was restricted [8]. Finally, a simulation of the pressure vessel was executed in the calibrated anisotropic composite material and another in steel, to extract the tangential and longitudinal stresses of both in order to compare the behavior of the two models [9].

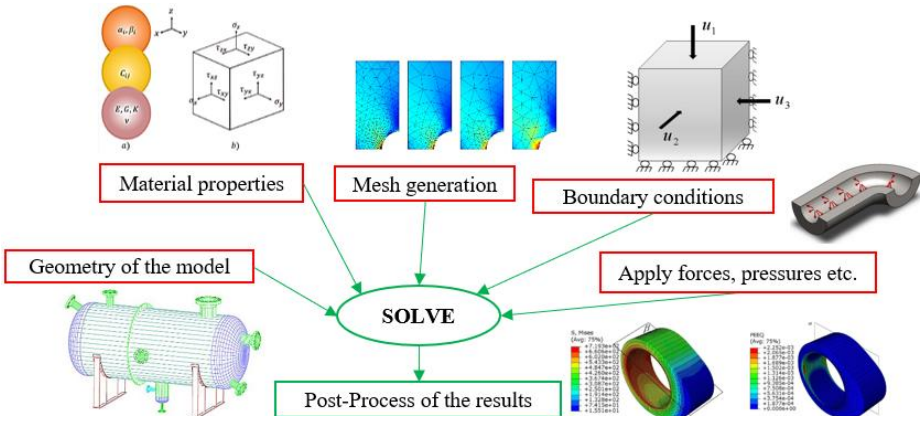

Figure 1: Free-body diagram of a thin-walled cylindrical pressure vessel with principal stresses; (a) internal pressure, (b) tangential stress, (b) longitudinal stress [10].

The focus of this analysis on linear elastic analysis of hoop and longitudinal stresses that develop in the cylindrical midzone of a thin-walled cylindrical pressure vessel. A container is analyzed that is commercial, widely used in different industrial areas, but that, in conventional materials such as steel, presents difficulties and generates economic losses due to maintenance stops [11].

The analysis starts from the assumption that a pressure vessel made of a composite material is more efficient than a vessel made of a simple homogeneous material such as steel. In order to have total control in the constitution of the anisotropic composite material to be used in the pressure vessel, the series/parallel mixing theory is used, with this theory it was possible to identify the anisotropy of the composite material caused by the orientation of the fibers and obtain the constitutive matrix.

To create a link between finite element numerical modeling and series/parallel mixing theory, the constitutive matrix of the anisotropic composite material is entered in APDL, obtaining a numerical model created with theoretical and simulated components. In conclusion, the purpose of this thesis is to propose a methodology that offers an exact control between the theoretical constitution of the anisotropic composite material using series/parallel mixing theory and finite element numerical modeling for stress analysis in cylindrical pressure vessels. thin-walled in composite material and simple homogeneous material.

II. MATERIALS AND METHODS

The methodology used for the development of this analysis consisted of the following steps:

I. Literature review concerning pressure vessels, shell membrane theory, constitutive equations of anisotropic materials, composite materials, study of series/parallel mixing theory for the design of composite materials, and finite element analysis in APDL.

II. Calibration of the 3-layer composite material with fiber orientations at +37°, -18°, -37°, using series/parallel mixing theory and validation using a simple numerical model.

III. Calibration of the results in the cylindrical coordinate system using the simple numerical model.

IV. Numerical modeling of the cylindrical pressure vessel with the calibrated composite material for comparison with the numerical model of a cylindrical pressure vessel made of simple homogeneous material.

To perform the calibration of the 3-layer composite material with fiber orientations at +37°, -37°, -18°, we began with the choice of two simple materials. Aluminum for the matrix with a volumetric participation of 60% and boron for the fibers with 40%. Next, the design process of the compound was carried out for the estimation of its anisotropic constitutive matrix, using the series/parallel mixture theory. To perform compatibility checks between the APDL finite element analysis tool and the theoretical stress estimation using series/parallel mixing theory, a link between them was created using the constitutive matrix of the compound. Said constitutive matrix is symmetric and describes an anisotropic behavior, therefore, its positions were entered in the input data of the preprocessor for APDL anisotropic materials.

For this calibration, the geometry of a beam of 10 mm in Z and 100 mm in X was created. A type of structural analysis, finite element type SHELL281 [13], was selected and a thickness of 3 mm was defined. A structured mesh of 20 finite elements (3 mm x 10 mm x 20 mm each) and 66 nodes was created. Then we proceeded to define the load and the restrictions in the nodes created with the mesh.

In nodes 1,2,23,35,45,57 the displacement in X, Y, Z was restricted to simulate a beam fixation, in node 46 which is located at the opposite end, a load was applied in Y of 10 N. Finally, the modeling was executed and the results were listed. To perform the extraction of the deformation vector, element 1 and node 2 of the same element were selected [14]. The strain vector extracted from the model was used as input data in the series/parallel mixture theory to theoretically estimate the stress vector, with the procedure exposed in chapter 2 from equations 2-91 to 2-117. These stresses were estimated for comparison with the stresses obtained from numerical modeling in APDL.In the cylindrical coordinate calibration of the results, a simple model consisting of a cylindrical ring was chosen. We started by choosing a structural analysis type, selecting the finite element type SHELL281, and entering the constitutive matrix of the designed 3-layer anisotropic composite material in the material calibration. Then, the geometry of the cylinder was created, which is 100 mm in height in Y x 200 mm in diameter in X, since it is a cylindrical geometry, the diameter was generated first and it was extruded in a parallel direction as an area. A distributed pressure load of 1 MPa was assigned to the cylinder areas and restraint confined the movement of the cylinder ends. In the module to define section, the previously defined composite material and the 2 mm thickness for the finite elements type SHELL281 were selected (figure2).

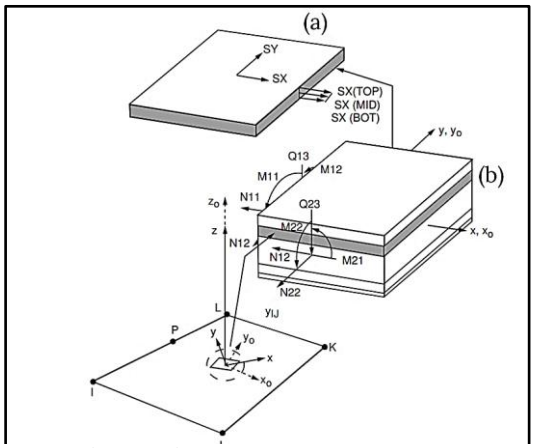

Figure 2: Description of results of the element shell281, (a) Thin shell; (b) Thick shell .

A structured mesh of 2160 elements and 2340 nodes was generated. Using the LOCAL 5 command, a Y-oriented cylindrical coordinate system was created (Chapter 2, Section 2-5), and using the ESYS 5 command, the coordinate system was assigned to each mesh element. The simulation of the model was executed, the element 185 and its node 2192 were chosen for the extraction of the main stresses, being the main stress 1 the so-called tangential stress and the main stress 2 the longitudinal stress. Subsequently, a theoretical estimate of the tangential and longitudinal stresses of the cylindrical geometry at a pressure of 1 MPa was made, for which the membrane theory for shells was used, since this cylinder meets the condition to use it. Finally, a comparison was made between the stresses obtained from the modeling and the stresses calculated theoretically.

As a result of the reliability generated by the calibrations, we proceeded with the modeling of the cylindrical pressure vessel. To start, a type of structural analysis was selected, SHELL281-type elements were chosen, a thickness of 6mm was defined for the shell-type elements, and the constitutive matrix of the calibrated anisotropic composite material was entered. For the geometry, the measurements used for commercial containers that store nitrogen at 15 MPa were chosen. The lines of a cut profile of the cylindrical container (oriented in Y) were created and revolved to create the areas. Next, the distributed pressure load of 15 MPa was defined in the vessel areas and the Y-direction displacement constraint was applied to the bottom base area of the vessel. It was necessary to generate a semi-structured mesh, this due to the change in geometry between the

filling nozzle and the central cylinder, so it was automatically generated and subsequently a refinement was performed. Using the LOCAL 5 command, a Y-oriented cylindrical coordinate system was created, and using the ESYS 5 command, the coordinate system was assigned to each mesh element. The simulation was run on the composite vessel to obtain the results and extract the principal stresses (figure 3). For the choice of the finite element, the numbering of these was generated, and an element was identified in the middle of the cylindrical area. At element 1602 and node 2922, hoop stress and longitudinal stress results were extracted for later comparison.

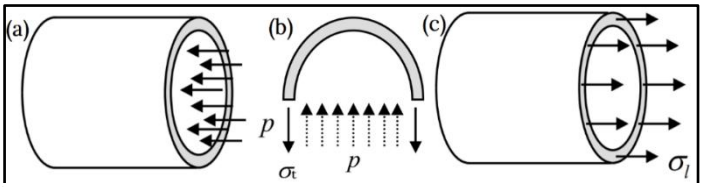

Figure 3:Free-body diagram of a thin-walled cylindrical pressure vessel with principal stresses; (a) internal pressure, (b) tangential stress, (b) longitudinal stress [23].

Next, for the model of the cylindrical pressure vessel in steel, the geometry and the same mesh created for the model in composite were used, the results of this model in homogeneous material were extracted in the same element and node. Using the membrane theory in shells for calculating stress in pressure vessels (figure 3) the tangential and longitudinal stress of the vessel at 15 MPa and given the geometry were calculated theoretically. We proceeded with the comparison of the results obtained from the model in calibrated composite material against the results in homogeneous steel material, and in turn with the results of the theoretical estimation. Finally, the weight of the steel container and the container made of composite material was calculated. To determine the weight of the composite container, the volume of the pressure container calculated in SolidWorks, the volumetric participation (boron 40% - aluminum 60%) and the densities were used. In the case of the steel container, this has a volumetric participation of 100%, so only its density and the volume of the container were needed.It is relevant to clarify that the volume that is treated in the methodology is the volume of material necessary to create the pressure vessel, that for the purpose of this analysis the important volume since it is the one occupied by the design material, distinguishing itself from the filling volume of the fluid that can store the pressure vessel.

2.1 Composite material design with series-parallel mixing theory

The procedure to obtain the constitutive equations of composite materials with the series/parallel mixture theory is based on the description of anisotropic surfacesthat limit the elastic domain. The solution adopted to consider the anisotropy of the component materials is based on the stress mapping concept [12].The anisotropic behavior of the material is formulated through a fictitious isotropic space of stresses and strains that is generated from a linear tensorial transformation of the real spaces of anisotropic stresses and strains [13].The series/parallel (SP) model considers that in a certain direction (or directions) the composite materials behave in parallel, while their behavior is serial in the other directions [14].This is done using two fourth-order projector tensors, one corresponding to the series direction (P_S) and the other projectorin the parallel direction (P_P). The strain is separated into its series and parallel components,

$$\varepsilon = \varepsilon_P + \varepsilon_S \tag{1}$$

With

$$\varepsilon_P = P_P : \varepsilon \text{ and } \varepsilon_S = P_S : \varepsilon \tag{2}$$

Whence,

$$P_S = I - P_P;\ P_P = N_P \otimes N_P \quad \text{and} \quad N_P = e_1 \otimes e_1 \tag{3}$$

Being the director vector that determines the parallel behavior of the fiber, it is the parallel projection tensor, and it is the identity. The stress state can be divided analogically, estimating its behavior in parallel and in series using the projecting tensors of fourth order P_p and P_s ,

$$\sigma = \sigma_P + \sigma_S \tag{4}$$

(5)

With $\sigma_P = P_P : \sigma$ and $\sigma_S = P_S : \sigma$

For each layer, the constitutive tensor is arranged in the local fiber coordinate system, then it is rotated to the global system and there the constitutive tensor of the composite is composed as shown in Figure 2-11.
The numerical model of the SP theory for the stress-strain state [73] is based on the following hypotheses:

1. The composite material has two main component parts: the fiber and the matrix. The component materials are assumed to have the same strain in the parallel (grain) direction.
2. The component materials have the same stress in the series direction.
3. The response of the composite material is directly related to the volumetric fractions of the simple materials that compose it.
4. Homogeneous distribution of phases is considered in the compound.
5. The perfect delimitation between components is also considered.

So, if an example composite material of 2 layers is analyzed, it can be said that each layer will have a volumetric share of the total composite, and each with its own orientation of the fibers as follows:

Layer 1: V_1 and layer 1 angle: α_1

Layer 2: V_2 and layer 2 angle: α_2

Simple fiber material properties E_f and v_f,

$$G_f = \frac{E_f}{2 \cdot (1 + \nu_f)} \tag{6}$$

Simple material properties of the matrix E_m and v_m,

$$G_m = \frac{E_m}{2 \cdot (1 + \nu_m)} \tag{7}$$

For the estimates, a transposed vector of imposed displacements can be used,

$$\varepsilon = \left[\varepsilon_{xx} \ \varepsilon_{yy} \ \varepsilon_{zz} \ \gamma_{xy} \ \gamma_{xz} \ \gamma_{yz} \right]^T \tag{8}$$

The constitutive tensor of the simple material of the matrix is found,

$$F_m = \begin{bmatrix} \frac{1}{E_m} & \frac{-\nu_m}{E_m} & \frac{-\nu_m}{E_m} & 0 & 0 & 0 \\ \frac{-\nu_m}{E_m} & \frac{1}{E_m} & \frac{-\nu_m}{E_m} & 0 & 0 & 0 \\ \frac{-\nu_m}{E_m} & \frac{-\nu_m}{E_m} & \frac{1}{E_m} & 0 & 0 & 0 \\ 0 & 0 & 0 & \frac{1}{G_m} & 0 & 0 \\ 0 & 0 & 0 & 0 & \frac{1}{G_m} & 0 \\ 0 & 0 & 0 & 0 & 0 & \frac{1}{G_m} \end{bmatrix} \tag{9}$$

Being C_m the constitutive matrix of the matrix material

$C_m = F_m^{-1}$

Using the parallel and series projector tensor, find the series and parallel components of the matrix from the parallel and series projectors:

(10)

$$P_P = [1\ 0\ 0\ 0\ 0\ 0]$$

$$P_s = \begin{bmatrix} 0 & 0 & 0 & 0 & 0 \\ 1 & 0 & 0 & 0 & 0 \\ 0 & 1 & 0 & 0 & 0 \\ 0 & 0 & 1 & 0 & 0 \\ 0 & 0 & 0 & 1 & 0 \\ 0 & 0 & 0 & 0 & 1 \end{bmatrix} \tag{11}$$

$$C_{mPP} = P_P \cdot C_m (P_P)^T \tag{12}$$

$$C_{mPS} = P_P \cdot C_m \cdot P_S \tag{13}$$

$$C_{mSP} = (P_S)^T \cdot C_m \cdot (P_P)^T \tag{14}$$

$$C_{mSS} = (P_S)^T \cdot C_m \cdot (P_s) \tag{15}$$

The constitutive tensor of the simple material of the fiber is found,

$$F_f = \begin{bmatrix} \frac{1}{E_f} & \frac{-\nu_f}{E_f} & \frac{-\nu_f}{E_f} & 0 & 0 & 0 \\ \frac{-\nu_f}{E_f} & \frac{1}{E_f} & \frac{-\nu_f}{E_f} & 0 & 0 & 0 \\ \frac{-\nu_f}{E_f} & \frac{-\nu_f}{E_f} & \frac{1}{E_f} & 0 & 0 & 0 \\ 0 & 0 & 0 & \frac{1}{G_f} & 0 & 0 \\ 0 & 0 & 0 & 0 & \frac{1}{G_f} & 0 \\ 0 & 0 & 0 & 0 & 0 & \frac{1}{G_{ff}} \end{bmatrix} \tag{16}$$

$$C_f = F_f^{-1} \tag{17}$$

$$C_{f\ PP} = P_P \cdot C_f (P_P)^T \tag{18}$$

$$C_{f\ PS} = P_P \cdot C_f \cdot P_S \tag{19}$$

$$C_{f\ SP} = (P_S)^T \cdot C_f \cdot (P_P)^T \tag{20}$$

$$C_{f\ SS} = (P_S)^T \cdot C_f \cdot (P_s) \tag{21}$$

Constitutive tensor of the composite material in local coordinates:
V_f ,volumetric participation of the fiber in the composite layer
V_m , volumetric participation of the fiber in the composite layer
Constitutive tensor of the composite material in local coordinates,

$$A = \left(V_f \cdot C_{m\ SS} + V_m \cdot C_{f\ SS}\right)^{-1} \tag{22}$$

$$C_{C\ PP} = (V_f \cdot C_{f\ PP} + V_m \cdot C_{m\ PP}) + V_f \cdot V_m ((C_{f\ PS} - C_{m\ PS}) \cdot A (C_{m\ SP} - C_{f\ SP})) \tag{23}$$

$$C_{C\ PS} = (V_f \cdot C_{f\ PS} \cdot A \cdot C_{m\ SS}) + (V_m \cdot C_{m\ PS} \cdot A \cdot C_{f\ SS}) \tag{24}$$

(25)

$$C_{C\,SP} = (V_m \cdot C_{f\,SS} \cdot A \cdot C_{m\,SP}) + (V_f \cdot C_{m\,SS} \cdot A \cdot C_{f\,SP})$$
$$C_{C\,SS} = V_1 \cdot ((C_{m\,SS} \cdot A \cdot C_{f\,SS}) + (C_{f\,SS} \cdot A \cdot C_{m\,SS})) \quad (26)$$

The constitutive matrix of the layer in local coordinate system is assembled with the estimated components,

$$C_{CL} = \begin{bmatrix} C_{PP} & C_{PS} & C_{PS} & C_{PS} & C_{PS} & C_{PS} \\ C_{SP} & C_{SS} & C_{SS} & C_{SS} & C_{SS} & C_{SS} \\ C_{SP} & C_{SS} & C_{SS} & C_{SS} & C_{SS} & C_{SS} \\ C_{SP} & C_{SS} & C_{SS} & C_{SS} & C_{SS} & C_{SS} \\ C_{SP} & C_{SS} & C_{SS} & C_{SS} & C_{SS} & C_{SS} \\ C_{SP} & C_{SS} & C_{SS} & C_{SS} & C_{SS} & C_{SS} \end{bmatrix} \quad (27)$$

From the application example that began to be developed in the equation, it is necessary to perform a coordinate transformation, for which the following procedure is used, α_1, is the orientation angle of the fibers of layer 1 of the composite.

$$L_1 = \cos(\alpha_1 \cdot \frac{\pi}{180°}) \quad (28)$$

$$L_2 = \sin(\alpha_1 \cdot \frac{\pi}{180°}) \quad (29)$$

$$L_3 = 0 \quad (30)$$

$$M_1 = \sin(\alpha_1 \cdot \frac{\pi}{180°}) \quad (31)$$

$$M_2 = \cos(\alpha_1 \cdot \frac{\pi}{180°}) \quad (32)$$

$$M_3 = 0; \quad N_1 = 0; \; N_2 = 0; \; N_3 = 0; \quad (33)$$

The coordinate transformation matrix is assembled,

$$T_1 = \begin{bmatrix} L_1^2 & L_2^2 & L_3^2 & 2\,x\,L_2\,x\,L_3 & 2\,x\,L_1\,x\,L_3 & 2\,x\,L_1\,x\,L_2 \\ M_1^2 & M_2^2 & M_3^2 & 2\,x\,M_2\,x\,M_3 & 2\,x\,M_1\,x\,M_3 & 2\,x\,M_1\,x\,M_2 \\ N_1^2 & N_2^2 & N_3^2 & 2\,x\,N_2\,x\,N_3 & 2\,x\,N_1\,x\,N_3 & 2\,x\,N_1\,x\,N_2 \\ M_1\,x\,N_1 & M_2\,x\,N_2 & M_3\,x\,M_3 & M_2\,x\,N_3 + M_3\,x\,N_2 & M_1\,x\,N_3 + M_3\,x\,N_1 & M_1\,x\,N_2 + M_3\,x\,N_1 \\ L_1\,x\,N_1 & L_2\,x\,N_2 & L_3\,x\,N_3 & L_2\,x\,N_3 + L_3\,x\,N_2 & L_1\,x\,N_3 + L_3\,x\,N_1 & L_1\,x\,N_2 + L_2\,x\,N_1 \\ L_1\,x\,M_1 & L_2\,x\,M_2 & L_3\,x\,M_3 & L_2\,x\,M_3 + L_3\,x\,M_2 & L_1\,x\,M_3 + L_3\,x\,M_1 & L_1\,x\,M_2 + L_2\,x\,M_1 \end{bmatrix} \quad (34)$$

For the following equations, the subscripts have the following meaning,

C, refers to the composite material.
G, the accompanying data is in global coordinates.
L, the accompanying data is in global coordinates.
S, means that the component is in parallel.
P, means that the component is in series.
m, refers to the parent material.
f, refers to the fiber material.

This transformation matrix is applied to the following equation to find the constitutive matrix of the shell composite in global coordinates C_{C1G},

$$C_{C1G} = T_1 \cdot C_{CL} \cdot T_1^T \quad (35)$$

For the second layer, the same procedure is carried out, but the different data is the orientation of the fiber, and the transformation matrix is obtained.
If there is a second layer, the constitutive matrix of the material in global coordinates of this second layer will be:

$$C_{C2G} = T_2 \cdot C_{CL} \cdot T_2^T \tag{36}$$

This same workflow should be used in case you have more layers.
The matrix of composite material, which for this example was 2 layers, is assembled with the two matrices that were estimated in global coordinates with the use of the transformation, with the volumetric participation that each layer has, as shown in the equation:

$$C_{CLG} = V_1 \cdot C_{C1G} + V_2 \cdot C_{C2G} + \cdots + V_n \cdot C_{CnG} \tag{37}$$

Having a strain vector, it is possible to estimate the stresses in the composite using the series/parallel mixing theory and its assumptions. The calculation of the deformation is carried out in the local coordinates of the laminate layers:

$$\varepsilon_{1G} = \varepsilon \tag{38}$$

$$\varepsilon_{1L} = T_1^T \cdot \varepsilon_{1G} \tag{39}$$

$$\varepsilon_{2G} = \varepsilon \tag{40}$$

$$\varepsilon_{2L} = T_2^T \cdot \varepsilon_{2G} \tag{41}$$

The decomposition of the deformations into series and parallel components is carried out,

$$\varepsilon_{C1P}: \tag{42}$$

$$\varepsilon_{C1P} = P_P \cdot \varepsilon_{1L} \tag{43}$$

$$\varepsilon_{C1S} = P_S^T \cdot \varepsilon_{1L} \tag{44}$$

The calculation of the parallel deformations of the matrix and of the layer fiber is carried out,

$$\varepsilon_{f1P}: \tag{45}$$

$$\varepsilon_{m1P} = \varepsilon_{C1P} \tag{46}$$

$$\varepsilon_{f1P} = \varepsilon_{C1P} \tag{47}$$

A prediction of the series strains for the layer matrix $\varepsilon_{m1S}{}^T$ and fiber is estimated,

$$\varepsilon_{f1S}{}^T: \tag{48}$$

$$\varepsilon_{m1S}{}^T = A \cdot (C_{fSS} \cdot \varepsilon_{C1S} + V_f (C_{fSP} - C_{mSP}) \cdot \varepsilon_{C1P}) \tag{49}$$

$$\varepsilon_{f1S}{}^T = \frac{\varepsilon_{C1S}}{V_f} - \frac{V_m}{V_f} \varepsilon_{m1S} \tag{50}$$

We proceed with a recompositing of the deformations of the matrix and fiber of the layer,

$$\varepsilon_{f1}{}^T: \tag{51}$$

$$\varepsilon_{m1}{}^T = P_P{}^T \cdot \varepsilon_{m1P} + P_S \cdot \varepsilon_{m1S} \tag{52}$$

$$\varepsilon_{f1}{}^{T} = P_P{}^{T} \cdot \varepsilon_{f1P} + P_S \cdot \varepsilon_{1S} \tag{53}$$

After having obtained the series and parallel components of the strains for the layer fiber and matrix, the stresses in the fiber and matrix can be estimated as follows:

$$\sigma_{m1}{}^{T} = C_m \cdot \varepsilon_{m1} \tag{54}$$

$$\sigma_{f1}{}^{T} = C_f \cdot \varepsilon_{f1} \tag{55}$$

$$\sigma_{m1P} = P_P \cdot \sigma_{m1} \tag{56}$$

$$\sigma_{f1P} = P_P \cdot \sigma_{f1} \tag{57}$$

$$\sigma_{m1S} = P_S{}^{T} \cdot \sigma_{m1} \tag{58}$$

$$\sigma_{f1S}{}^{T} = P_S{}^{T} \cdot \sigma_{f1} \tag{59}$$

Then a verification of the isostress hypothesis is performed,

$$\text{error} = \left|\sigma_{m1S} - \sigma_{f1S}\right| \tag{60}$$

$$\text{Re error1} = \frac{\text{error}}{\left|P_S{}^{T} \cdot \sigma_{m1}\right|} \tag{61}$$

$$\text{Re error2} = \frac{\text{error}}{\left|P_S{}^{T} \cdot \sigma_{f1}\right|} \tag{62}$$

Now the stresses in layer 1 can be calculated like this,

$$\sigma_{C1P} = V_m \cdot \sigma_{m1P} + V_f \cdot \sigma_{f1P} \tag{63}$$

$$\sigma_{C1S} = \sigma_{m1S} \tag{64}$$

$$\sigma_{C1L} = P_P{}^{T} \cdot \sigma_{C1P} + P_S \cdot \sigma_{C1S} \tag{65}$$

$$\sigma_{C1G} = T_1 \cdot \sigma_{C1L} \tag{66}$$

This procedure is carried out for the layers that make up the composite, if two layers are assumed, finally the global effort would be:

$$\sigma = V_1 \cdot \sigma_{C1G} + V_2 \cdot \sigma_{C2G} \tag{67}$$

In the same way, the same procedure is followed to estimate the composite if more layers are placed in the design,

$$\sigma = V_1 \cdot \sigma_{C1G} + V_2 \cdot \sigma_{C2G} \cdots V_n \cdot \sigma_{CnG} \tag{68}$$

For a case of elastic analysis, the stress obtained with this procedure coincides with the predictor stress found from the constitutive tensor of the compound shown in Equation 2-96,

$$\{\vec{\sigma}\} = C_{LG} \cdot \{\vec{\varepsilon}\} \tag{69}$$

The composite material designed with the theory of parallel series mixtures from two simple materials, has the behavior of an anisotropic material of the form,

$$\begin{Bmatrix} \varepsilon_{xx} \\ \varepsilon_{yy} \\ \varepsilon_{zz} \\ \gamma_{xy} \\ \gamma_{xz} \\ \gamma_{yz} \end{Bmatrix} = \begin{bmatrix} C_{11}^{-1} & C_{12}^{-1} & C_{13}^{-1} & 0 & 0 & C_{16}^{-1} \\ C_{21}^{-1} & C_{22}^{-1} & C_{23}^{-1} & 0 & 0 & C_{26}^{-1} \\ C_{31}^{-1} & C_{32}^{-1} & C_{33}^{-1} & 0 & 0 & C_{36}^{-1} \\ 0 & 0 & 0 & C_{44}^{-1} & C_{45}^{-1} & 0 \\ 0 & 0 & 0 & C_{54}^{-1} & C_{55}^{-1} & 0 \\ C_{61}^{-1} & C_{62}^{-1} & C_{63}^{-1} & 0 & 0 & C_{66}^{-1} \end{bmatrix} \cdot \begin{Bmatrix} \sigma_{xx} \\ \sigma_{yy} \\ \sigma_{zz} \\ \tau_{xy} \\ \tau_{xz} \\ \tau_{yz} \end{Bmatrix} \tag{70}$$

III. RESULTS AND DISCUSS

3.1 Composite material designed with series-parallel mixing theory

The composite material designed with the series-parallel mixture theory is presented in the following constitutive matrix (table 1),

Table 1: Matrix of the calibrated composite material

Symbols	Values (MPa)					
Cc	1,79E+05	6,34E+04	4,65E+04	0	0	8,51E+03
	6,34E+04	1,39E+05	5,10E+04	0	0	3,14E+01
	4,65E+04	5,10E+04	1,35E+05	0	0	-9,69E+02
	0	0	0	4,07E+04	-4,85E-12	0
	0	0	0	-4,85E-12	4,07E+04	0
	8,51E+03	3,14E+01	-9,69E+02	0	0	6,03E+04

3.2 Numerical model for calibration

In Ansys Parametric Design Language, it was carried out in a simple beam model, embedded at one end and with a force applied at the opposite end. In the material definition module, the constitutive matrix of the designed anisotropic material was entered, a structured mesh was created, and the deformation vector was extracted at one of the finite element nodes to use it with the equation and theoretically estimate the stresses and so on compare them with the efforts obtained from the modeling in APDL (figure 4).

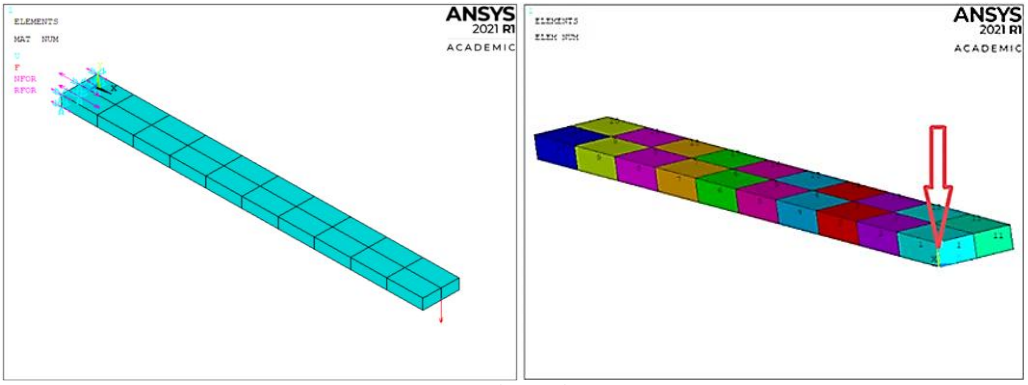

Figure 4: Model of beam for calibration.

The result of the deformation due to the imposed load is the expected one as seen in the figure. The stress distribution is presented in part b of the figure 5, showing in red the place where the greatest stress occurs.

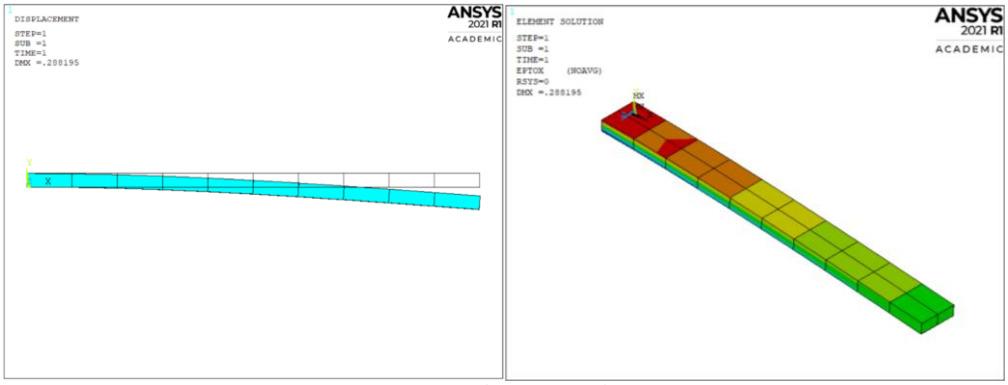

Figure 5: Designation of the selected finite element.

The strain vector was extracted from one of the nodes of the selected finite element, as APDL performs an internal process of extrapolation of the results of the Gaussian points to the nodes, it is reliable to use such data and is show in the table 2.

Table 2: Matrix of the calibrated composite material

Descripción	Símbolo	Valor	Unidad
Strain in X	ε_{xx}	-8,335E-05	--
Strain in Y	ε_{yy}	4,17E-05	--
Strain in Z	ε_{zz}	4,17E-05	--
Shear strain in XY	γ_{xy}	-4,38E-04	--
Shear strain in XZ	γ_{xz}	1,87E-05	--
Shear strain in YZ	γ_{yz}	0	--

The efforts resulting from the numerical modeling were also removed, since these were necessary to compare them with the theoretical results estimated with the series-parallel mixture theory, are show in the table.
The theoretically estimated stresses with the series-parallel mixture theory were found with the procedure set from in the equations .The error percentage (equation 62) was also estimated and it was verified that the error percentages between the theoretical efforts with SP and the numerical modeling efforts were acceptable, and this reliability allowed using the material designed for the main model of the pressure cylinder.

Table 3: Stresses resulting from modeling in ADPL

Description	Symbol	Value	Unit
Stress in X	σ_{xx}	-10,18	MPa
Stress in Y	σ_{yy}	2,63	MPa
Stress in Z	σ_{zz}	3,86	MPa
Shear stress in XY	τ_{xy}	-17,83	MPa
Shear stress in XZ	τ_{xz}	0,38	MPa
Shear stress in YZ	τ_{yz}	0	MPa

Table 4: Stresses resulting from modeling in ADPL

Description	Symbol	Value	Unit
Stress in X	σ_{xx}	-10,14	MPa
Stress in Y	σ_{yy}	2,66	MPa
Stress in Z	σ_{zz}	3,88	MPa
Shear stress in XY	τ_{xy}	-17,85	MPa
Shear stress in XZ	τ_{xz}	0,40	MPa
Shear stress in YZ	τ_{yz}	0	MPa

Table 6: Stresses resulting from modeling in ADPL

Symbol	(%)
σ_{xx}	0,20
σ_{yy}	1,13
σ_{zz}	0,52
τ_{xy}	0,11
τ_{xz}	2,56
τ_{yz}	0

3.3 Stress estimation in a cylindrical pressure vessel made of composite material versus a steel vessel

A geometry used in nitrogen transport was chosen, and a semi-structured mesh was made to apply the internal pressure of 15 Mpa.

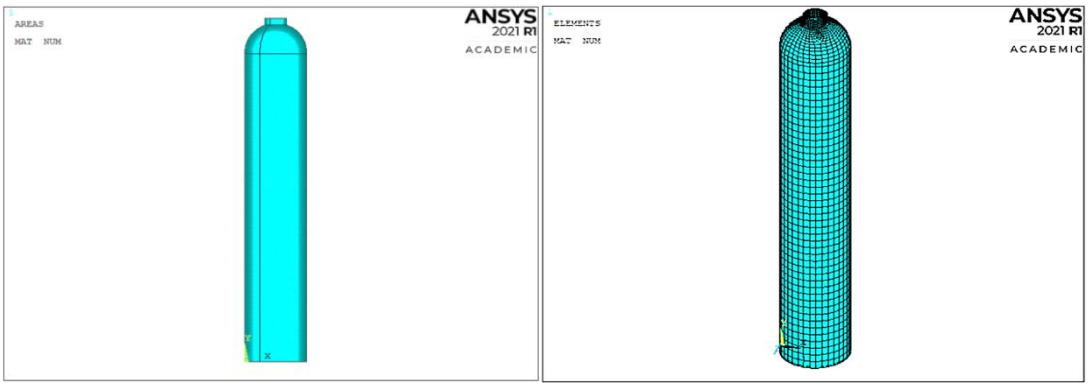

Figure 6: Pressure vessel model and semi-structured mesh.

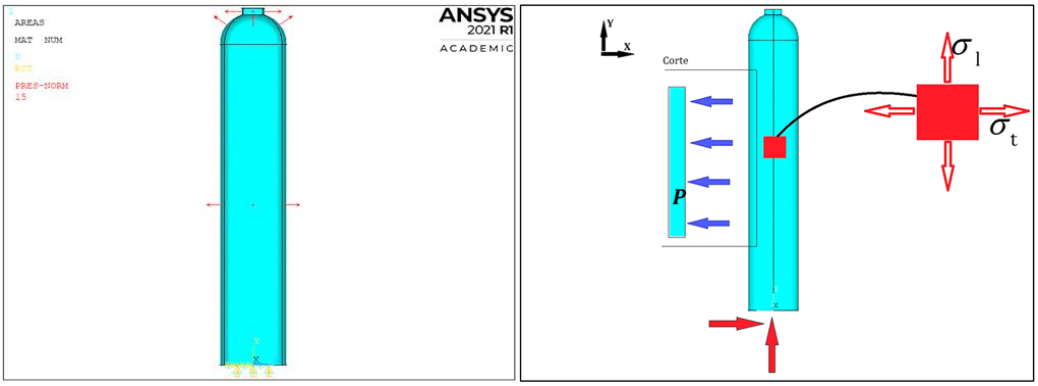

Figure 7: Boundary conditions.

Using the equations, the hoop stress and the longitudinal stress were estimated theoretically for comparison with the results in the numerical modeling.

$$\sigma_t = \frac{(15\ \text{MPa} \cdot 109\ \text{mm})}{6\ \text{mm}} = 272.5\ \text{MPa} \ ; \ \sigma_l = \frac{(15\ \text{MPa} \cdot 109\ \text{mm})}{(2 \cdot 6\ \text{mm})} = 136.3\ \text{MPa}$$

The displacement of the initial position of the cylinder and of the final position due to the pressure can be seen in the figure, as the distribution of the effort is shown, blue to show the beginning of the effort and orange-red to show where the effort increased.

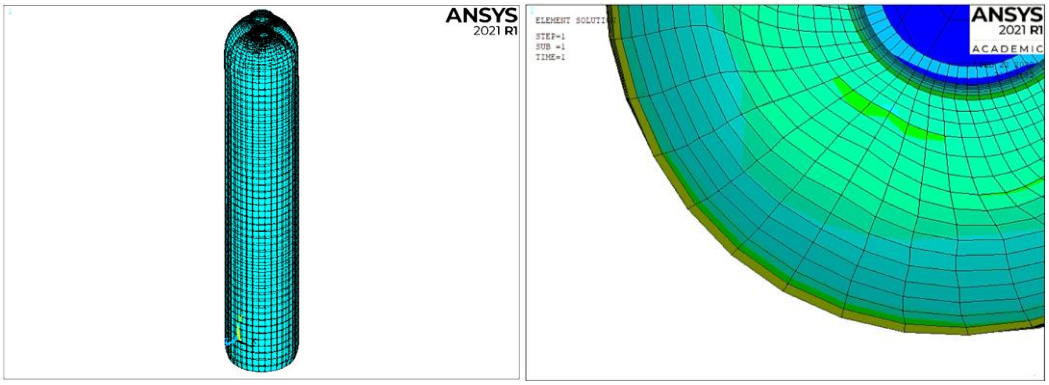

Figure 8: pressure vessel model and semi-structured mesh.

The results of the modeling of the pressure vessel in the calibrated composite material are presented in the table,

Table 7: Stresses resulting from modeling in ADPL

Name	Description	Symbol	Value	Unit
Composite material pressure vessel	Hoop stress	σ_t	219.4	MPa
	Longitudinal stress	σ_l	93.0	MPa

The modeling of the pressure vessel made only of steel was also carried out, this was later compared with the modeling in composite material. Next table presents the hoop and longitudinal stresses of the steel pressure vessel:

Table 8: Stresses resulting from modeling in ADPL.

Name	Description	Symbol	Value	Unit
Steel material pressure vessel	Hoop stress	σ_t	280.23	MPa
	Longitudinal stress	σ_l	123.16	MPa

Finally, the weight of the steel pressure vessel and the composite pressure vessel was estimated. The pressure vessel has the same volume for both models, only the type of material changes.

Table 9: Weight of the Steel pressure vessel

Description	Volume (m^3)	Density (kg/m^3)	Mass (kg)
Acero	0.048	7850	376.8

In the case of the pressure vessel, the volume percentage of aluminum is the same percentage used in the design of the composite material, also for the fibers.

Tabla 10: Weight of the pressure vessel in composite material

Description	Volume (m^3)	Density (kg/m^3)	Mass (kg)
Aluminum (60 %)	0,0288	2700	77.76
Boron (40 %)	0.0192	2460	47.23

After obtaining the weights related to the steel pressure vessel, and the composite material pressure vessel, a percentage comparison is made, this is necessary to know what percentage of decrease there is when using an composite pressure vessel compared to conventional steel.

Tabla 11:Comparison of the mass of the two models with percentage of weight reduction.

Description	Mass (kg)	Mass reduction	Reduction percentage (%)
Acero	376,8	251.8	67
Aluminio/boro	125		

From the tangential and longitudinal stresses obtained in the model of steel and composite material, it was evident that the cylindrical pressure vessel made in the designed composite material influences a reduction in stress, this means that the model in composite material is more mechanically efficient than the steel model. Next table presents the estimate of the reduction of the model in composite compared to the results of the model in steel:

Table 12: Difference of efforts between the model of composite material or model of Steel.

Description	Value (MPa)	Composite vs Steel Comparison
Hoop stress for composite	219,4	60,83
Hoop stress for steel	280,23	
Longitudinal stress for composite	93	30,16
Longitudinal stress for steel	123,16	

It is evident how the container made of anisotropic composite material provides great resistance to tangential stress compared to steel.

IV. CONCLUSION

This study was an exercise in numerical modeling versus theoretical estimation using the series-parallel mixture theory and the membrane shell theory. Next, the conclusions related to the great steps taken to carry out the parameter calibrations and finally the modeling of the cylindrical pressure vessel in composite material and steel are presented.With the calibration models, it was checked that the units entered and the units of the results were consistent. The design of the composite material with the theory of series/parallel mixtures required that at least two mechanical properties of two simple materials be known in units such as MPa for Young's modulus and dimensionless for Poisson's ratio. Finally, it was verified that the stress results in the post-process coincide with these units.From the design of the composite material (+37°,-37°,18°) using the series/parallel mixture theory, the constitutive matrix of said composite was extracted, this constitutive matrix represented the behavior of a monoclinic anisotropic material, that is, of 13 constants, then this matrix was entered into APDL manually in the material definition step where the option of anisotropic materials was selected, that is, this was the link step between the series/parallel mixture theory and the numerical model.APDL allowed the input of the constitutive matrix of the composite material after calculating its constitutive matrix as an anisotropic material.With the calibrations carried out in APDL, it was verified that the SHELL281 type elements have the capacity to model anisotropic materials, in addition to working for thin-walled geometries such as that of the modeled pressure vessel.The results obtained by carrying out the theoretical estimation with the shell membrane theory were possible due especially to the fact that the selected geometry complied with the thin wall conditions. These conditions allow estimates of only principal stresses in the pressure vessel wall, which means that due to the orientation of the pressure vessel, only longitudinal stresses were present in the Y direction and tangential stresses in the X direction, but in Z. no efforts are presented, which was verified from the numerical modeling as well. The reduction percentage between the numerical modeling and the theoretical estimation for the tangential stresses was 60.83 MPa, and for the longitudinal stresses it was 30.16 MPa, which represents a great contribution of resistance of the anisotropic composite material designed by means of the SP theory.

REFERENCES

[1]. M. D. Actis and J. P. Durruty, "Handout - Structures IV - Analysis of Cylindrical Structures: Thin-Walled Cylinders Subjected to Compression and Internal Pressure." Faculty of Engineering National University of La Plata, La Plata, pp. 20–30, 2009.

[2]. J. J. Skrzypek and A. W. Ganczarski, Mechanics of Anisotropic Materials. Switzerland: Springer, 2015.

[3]. M. A. Savi, "Continuum Mechanics," Dyn. Smart Syst. Struct. Concepts Appl., no. November 2017, 2016, doi: 10.1007/978-3-319-29982-2.

[4]. X. Martinez, "Micro Mechanical Simulation of Composite Materials Using the Serial / Parallel Mixing Theory," Universidad Politécnica de Cataluña, 2008.

[5]. F. Rastellini, S. Oller, and E. Oñate, Numerical modeling of constitutive non-linearity of composite laminates. Barcelona: International Center for Numerical Methods in Engineering, 2007.

[6]. J. A. Paredes, "Modelización numérica del comportamiento constitutivo del daño local y global y su correlación con la evolución de las frecuencias naturales en estructuras de hormigón reforzado," Universidad Politécnica de Cataluña, 2013.

[7]. X. Martinez, S. Oller, and E. Barbero, "Characterization of delamination in composite materials using series/parallel mixing theory," Rev. Int. Metod. number for Calc. and Disen. in Eng., vol. 27, no. 3, p. 189–199, 2011, doi: 10.1016/j.rimni.2011.07.001.

[8]. D. Kim, Solid Mechanics: Anisotropic elasticity. 2020.

[9]. A. P. S. Selvadurai and H. Nikopour, "Transverse elasticity of a unidirectionally reinforced composite with an irregular fibre arrangement: Experiments, theory and computations," Compos. Struct., vol. 94, no. 6, pp. 1973–1981, 2012, doi: 10.1016/j.compstruct.2012.01.019.

[10]. B. Ren, J. Noda, and K. Goda, "Effects of fiber orientation angles and fluctuation on the stiffness and strength of sliver-based green composites," J. Soc. Mater. Sci. Japan, vol. 59, no. 7, pp. 1–9, 2010, doi: 10.2472/jsms.59.567.

[11]. E. M. Alawadhi, Finite Element Simulations Using ANSYS. Broken Sound Parkway: CRC Press Taylor & Francis Group, 2010.

[12]. E. I. Celis Imbajoa, "Nonlinear behavior of slabs composed of collaborating sheet, with and without conventional reinforcement. Experimental and numerical modeling.," Universidad Nacional de Colombia Sede Manizales, 2020.

[13]. ANSYS, Theory Reference for the Mechanical APDL and Mechanical Applications, 12th ed., vol. 3304, no. April. Canonsburg: Ansys Icn, 2009.
[14]. E. J. Barbero, Introduction to Composite Materials Design, 2nd ed. UP Catalunya: CRC Press Taylor & Francis Group, 2010.